*Int. J. Electrochem. Sci.*, 10 **(2015)** 3088 - 3097

International Journal of
ELECTROCHEMICAL
SCIENCE
www.electrochemsci.org

*Short Communication*

# Synthesis, Characterization and Electrocatalytic Activity of Silver Doped-Titanium Dioxide Nanoparticles

*Samira Bagheri*[1,*], *Donya Ramimoghadam*[1], *Amin Termeh Yousefi*[2], *Sharifah Bee Abd Hamid*[1]

[1]Nanotechnology & Catalysis Research Centre (NANOCAT), IPS Building, University of Malaya, 50603 Kuala Lumpur, Malaysia
[2]ChECA IKohza, Dept. Environmental & Green Technology (EGT), Malaysia Japan International Institute of Technology (MJIIT), University Technology Malaysia (UTM), Kuala Lumpur, Malaysia
[*]E-mail: samira_bagheri@um.edu.my

*Received:* 3 November 2014 / *Accepted:* 18 December 2014 / *Published:* 24 February 2015

This work reports the green synthesis of silver doped-titanium dioxide (Ag-$TiO_2$) which was carried out in aqueous gelatin solution. The Ag-$TiO_2$ nanoparticles were characterized with transmission electron microscopy (TEM), voltammetric and spectroscopic techniques i.e. X-ray diffraction (XRD), energy-dispersive X-ray (EDX) and Fourier transform-infrared (FT-IR). The results from XRD indicated pure Ag-$TiO_2$ and $TiO_2$ powders in anatase phase with an average crystallite size of 11 nm and 15 nm, respectively. However, Ag doped in $TiO_2$ did not significantly affect the crystalline structure of $TiO_2$. An efficient Ag-$TiO_2$-based anode was fabricated by casting a solution of the synthesized Ag-$TiO_2$ on glassy carbon electrode (Ag-$TiO_2$/GCE). Linear scanning voltammetry (LSV) in alkaline media was performed to investigate the electrocatalytic performance of Ag-$TiO_2$/GCE towards oxygen evolution reaction (OER). The OER is significantly enhanced at the Ag-$TiO_2$/GCE, evidenced by a negative shift in the LSV curve of Ag-$TiO_2$/GCE compared to the curve obtained at the unmodified electrode. The energy-savings value of oxygen gas at a current density of 7 mA $cm^{-2}$ was calculated as 14.4kWh $kg^{-1}$. The cost-effectiveness and stability of the modified electrode make it a potential design for application in the industrial water electrolysis process.

**Keywords:** Silver doped titanium dioxide nanoparticles, Gelatin, Oxygen evolution reaction, Electrocatalyst.

## 1. INTRODUCTION

Titanium dioxide ($TiO_2$) is a semiconducting oxide which finds application in a variety of industrial applications due to its non-toxicity, relative abundance and resistance to corrosion**.** $TiO_2$ exhibits remarkable properties such as hydrophilicity [1] as well as antibacterial [2] and self-cleaning

[3] activity. Due to its optical activity [4], $TiO_2$ is often used in photocatalytic decomposition [5] and more recently as a photocatalyst for the reduction of $CO_2$ to methanol [6].

There are many approaches to synthesize $TiO_2$ and modified $TiO_2$ [7] including hydrothermal [8], electrochemical [9], microwave [10], sonochemical [11] and sol-gel methods [12]. Among these methods, the sol-gel method offers simple methodology, high control of surface area, average crystallite size, phase structure and morphology. All of these parameters determine the photocatalytic activity of $TiO_2$.

Considerable research has been carried out to improve the electrocatalytic and photocatalytic activity of $TiO_2$, with reported methods such as metal ion doping [13], non-metal ion doping [14], co-doping [15] and exposed reactive anatase [001] facet [16]. Transition metals doped on $TiO_2$ play the role of charge carrier trap, which allows for light absorption in the visible range and enhances surface electron excitation by visible-light excited plasmon resonance [17-19]. Thus transition-metal doping on $TiO_2$ results in improved photocatalytic activity of $TiO_2$ nanocomposites.

Titania compounds doped with silver have been synthesized for antibacterial and photoelectrochemical applications [20, 21]. Indeed, $TiO_2$ doped with silver nanoparticles have shown improved photocatalytic activity compared with its undoped counterpart [22, 23]. It was proposed that Ag doping of $TiO_2$ improves charge transfer and charge pair separation efficiency [24].

The oxygen evolution reaction (OER) is a common reaction applied in fields of energy conversion, water-splitting and storage devices [25, 26]. The OER is often catalyzed using metal oxide-based anodes e.g. nickel and cobalt due to their notable stability and activity [27, 28]. Electrodes modified with nanoparticles were found to increase the surface area to volume ratio significantly and improve the electronic properties of the bare electrode [29, 30]. In this study, silver doped-$TiO_2$ (Ag-$TiO_2$) in anatase form was prepared via sol-gel method. The synthesized Ag-$TiO_2$ was then investigated for enhanced catalytic activity with regards to the oxygen evolution reaction.

## 2. EXPERIMENTAL PROCEDURE

### *2.1. Materials and apparatus*

Titanium tetraisopropoxide (TIPP) (98% purity) and silver(I) nitrate was purchased from Acros Organics and Allchem, respectively. Glacial acetic acid (100% purity) was purchased from Merck. Other analytical-grade reagents were purchased from Aldrich or Merck and used as received without further purification.

Electrochemical measurements were performed by a potentiostat/galvanostat (Autolab, Netherlands). A three-electrode system was used in all voltammetric experiments whereby a glassy carbon electrode coated with the synthesized Ag-$TiO_2$ samples was used as the working electrode. A silver-silver(I) chloride ($Ag \mid AgCl \mid KCl_{3M}$) electrode and platinum wire was used as the reference and auxiliary electrode, respectively (Metrohm). Elemental analysis and chemical characterization of the sample was carried out using energy-dispersive X-ray (EDX) spectroscopy (INCA Energy 400, Oxford Instruments). Powder X-ray diffraction (XRD) was used to identify the crystal phase and estimate

crystal size (Bruker-D8). Transmission electron microscopy (TEM) images of the Ag-$TiO_2$ nanoparticles were obtained using LEO-Libra 120 microscope. A BRUKER FT-IR spectrometer was used for Fourier transform infrared spectroscopy (FT-IR) studies.

### *2.2. Synthesis of Ag-doped $TiO_2$ nanoparticles*

To prepare the precursor solution, titanium tetraisopropoxide (TIPP), glacial acetic acid (AA) and deionized water ($H_2O$) were mixed in the mentioned order using a TIPP:AA:$H_2O$ with molar ratio of 1:10:200 [31]. Three gram gelatin was dissolved in 100 mL of deionized water, stirring at 60°C for 30 minutes and was added to TIPP precursor solution under vigorous stirring. Then 10 mL silver nitrate solution (0.1M) was added drop wise to this solution. The solution was dried at 80°C overnight. The dried gel was then ground to a fine powder and calcined in a muffle furnace at 500°C for 5 hours.

### *2.3. Fabrication of Ag-$TiO_2$/GCE*

Prior to the working electrode modification, a bare glassy carbon electrode (GCE) was cleaned by polishing the electrode surface on chamois leather with 0.05μm alumina powder. The GCE was then sonicated in deionized water and absolute ethanol, respectively. A dispersed solution of the synthesized Ag-$TiO_2$ nanoparticles was prepared by sonicating 1mg of the sample in 5mL absolute ethanol. The cleaned GCE was coated by casting 5μL of the Ag-$TiO_2$ solution and dried at room temperature to allow solvent evaporation.

## 3. RESULTS AND DISCUSSION

### *3.1. Powder X-ray diffraction study*

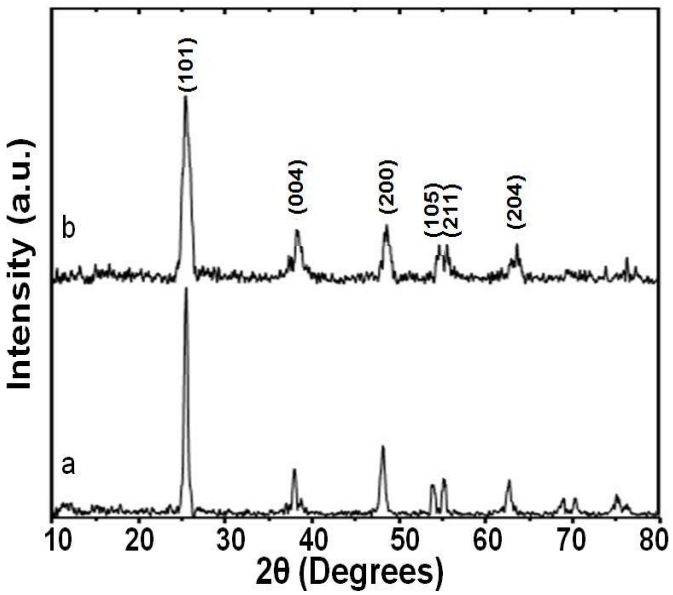


**Figure 1.** XRD patterns of (a) Ag-$TiO_2$ and (b) $TiO_2$ nanoparticles.

The XRD patterns of $TiO_2$ and Ag-$TiO_2$ powders which were calcined at 500°C in air for 5 hours are shown in Figure 1. The wide-angle XRD pattern showed anatase-phase $TiO_2$ with characteristic diffraction peaks of 2θ values at about 25.6(101), 38.1(004), 48.5(200), 54.7(105), 55.3(211), 63.0(204), 68.9(116), 70.8(220) and 76.1(215), respectively. Thus the prepared Ag-$TiO_2$ (pattern a) and $TiO_2$ (pattern b) powders were well-crystallized pure anatase form. The average particle sizes of pure Ag-$TiO_2$ and $TiO_2$ powders for the (101) plane were approximately 11 and 15 nm, respectively. This was based on the full-width half maximum measurement at 2θ of the maximum diffraction peak using Scherrer's formula (1),

$$D=K\lambda/\beta\cos\theta \quad (1)$$

In this equation, D is the crystallite size, K the Scherrer constant usually taken as 0.89, λ the wavelength of the X-ray radiation (0.15418nm for Cu Kα). Comparing the XRD patterns of pure $TiO_2$ to Ag-$TiO_2$, it appears that Ag loading does not significantly influence the crystalline structure of $TiO_2$. Ag phase was not detected in the XRD patterns of Ag-$TiO_2$ powders, perhaps due to insufficient Ag content to form observable crystalline structures.

*3.2. FT-IR studies*

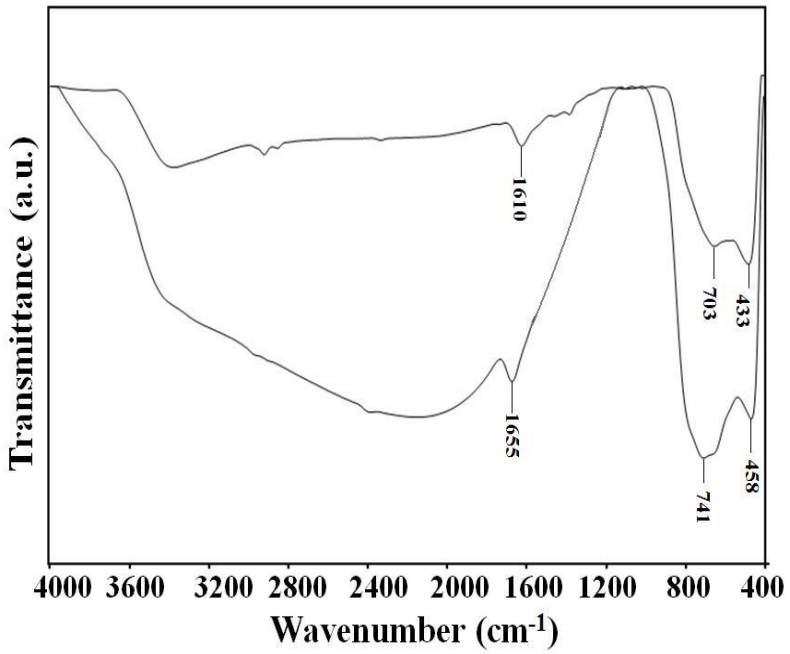


**Figure 2.** FT-IR patterns of (a) $TiO_2$ and (b) Ag-$TiO_2$ nanoparticles.

Figure 2 illustrates the FT-IR spectra of $TiO_2$ (curve a) and Ag-$TiO_2$ (curve b) nanoparticles which were synthesized by sol-gel method. The peaks at 433 and 703 $cm^{-1}$ observed in undoped $TiO_2$ sample correspond to O-Ti-O bonding [32]. Ti-O and O-Ti-O- flexion vibration give rise to the broad absorption bands at 400 $cm^{-1}$ and 800 $cm^{-1}$. The band centered at 1610 $cm^{-1}$ is characteristic of $\delta H_2O$ bending. The vibration bands between 1300 $cm^{-1}$ and 4000 $cm^{-1}$ can be attributed to the chemisorption

and/or physisorption of $H_2O$ and $CO_2$ molecules on the surface of the compound. Both doped and undoped $TiO_2$ exhibit similar vibration patterns.

### *3.3. TEM and EDX*

TEM micrographs of $TiO_2$ and Ag-$TiO_2$ are displayed in Figure 3. Similar morphology can be observed for the $TiO_2$ (image a) and Ag-$TiO_2$ (image b) samples. However, the TEM images indicate smaller particle sizes of Ag-$TiO_2$ compared to $TiO_2$. Energy dispersive X-ray spectroscopy (EDX) of Ag-$TiO_2$ indicates the presence of Ti, O and Ag with 60.53, 34.33 and 5.14 weight percent respectively (Figure 4).

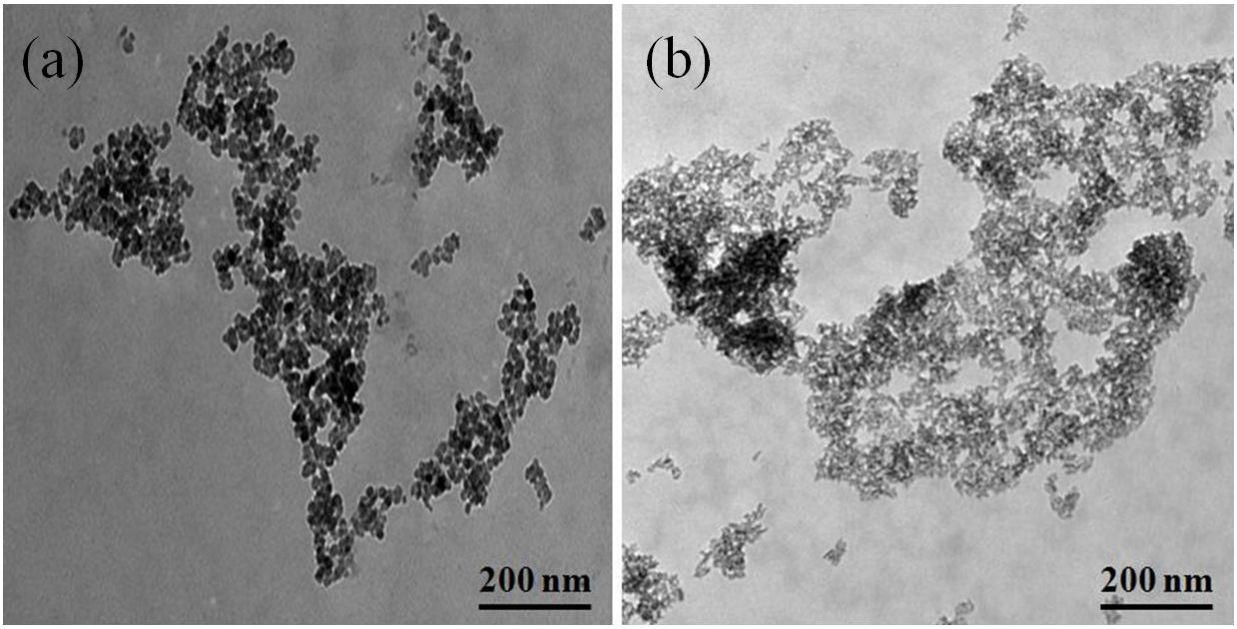


**Figure 3.** TEM images of (a) $TiO_2$ and (b) Ag-$TiO_2$ nanoparticles.

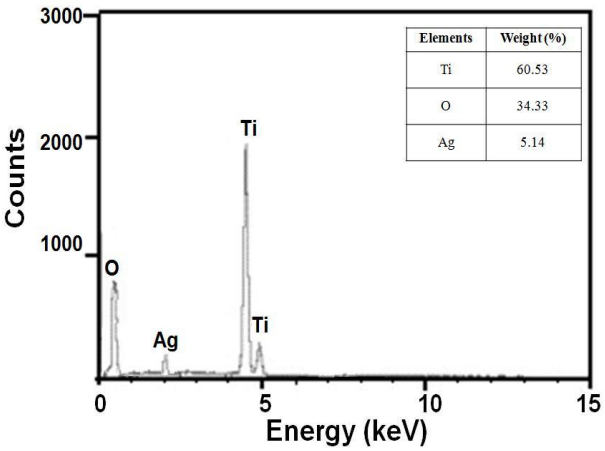


**Figure 4.** EDAX pattern of Ag-$TiO_2$ nanoparticles.

### *3.4. Electrochemical behavior of Ag-$TiO_2$/GCE*

Cyclic voltammetry is commonly used in electrochemistry to determine electroactivity performance. Figure 5 shows the cyclic voltammetric response obtained at the Ag-$TiO_2$/GCE in 0.1M KOH. Figure 5 indicates a series of anodic events which attribute to oxidation of $Ag \rightarrow Ag^+$ for Ag-$TiO_2$/GCE at a scan rate of 50 mV $s^{-1}$ which is in agreement with results from literature [33, 34]. The surface concentration of the electroactive Ag on Ag-$TiO_2$/GCE, $\Gamma$ (in mol/$cm^2$), is estimated using the equation [35]:

$$\Gamma = Q/nFA \quad (1)$$

Whereas Q is the value of charge consumed measured in Coulombs. Q is obtained from cyclic voltammograms by integrating the area under the anodic (or cathodic) peak curve with background correction. The average $\Gamma$ value of $(7.36 \pm 0.54) \times 10^{-11}$ mol/$cm^2$ was obtained. The stability of the Ag-$TiO_2$/GCE was tested by consecutive cyclic voltammetry of Ag-$TiO_2$/GCE by cycling potential in the range of -0.4 to 1.4 eV. Very slight activity variation was observed even after 20 cycles indicating Ag-$TiO_2$ stability in KOH medium.

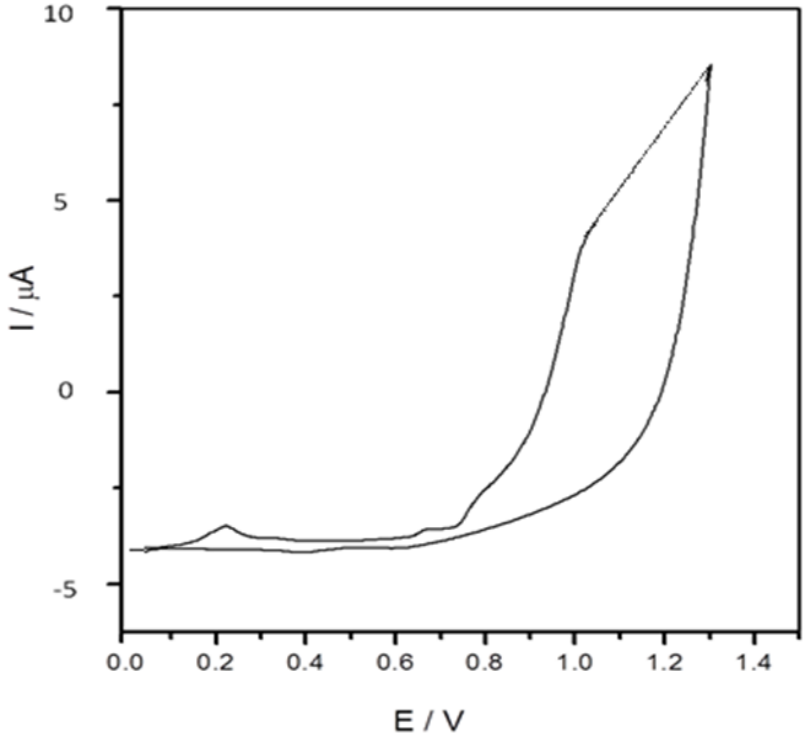


**Figure 5.** Cyclic voltammogram of Ag-$TiO_2$/GCE in 0.5 M KOH solution at scan rate 50 mV $s^{-1}$

### *3.5. Electrocatalytic activity of Ag-$TiO_2$ /GCE towards OER*

The electrocatalytic activity of the Ag-$TiO_2$ modified GCE was investigated by measuring the linear sweep voltammetry (LSV) in 0.1M KOH at a scan rate of 50 mV $s^{-1}$, as shown in Figure 6. This figure reveals a significant enhancement in the electrocatalytic activity towards the OER upon the modification of GCE with Ag-$TiO_2$. The onset potential of the OER was observed to shift towards the negative direction at the modified GCE. A significant decrease in the value of $E_5$ at the Ag-$TiO_2$ /GCE

can also be observed, compared to the unmodified electrode (GCE) in Figure 6. This indicates a significant enhancing role of Ag-$TiO_2$ towards the OER. This result corresponds to an equivalent decrease in the energy consumption accompanying the overall electrolysis process.

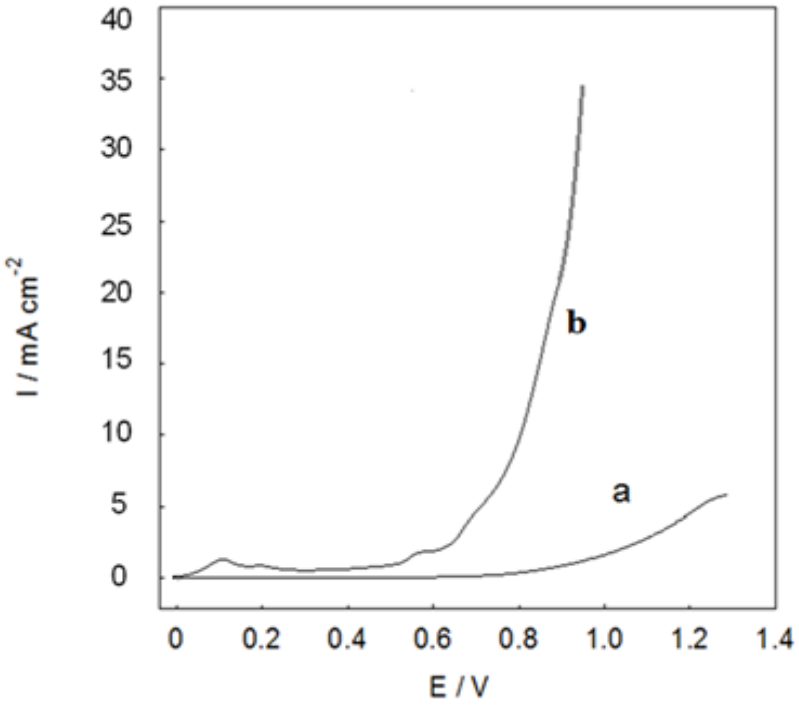


**Figure 6.** Linear sweep voltammograms of (a) bare GCE and (b) Ag-$TiO_2$/GCE in 0.5 M KOH at a scan rate of 50 mV $s^{-1}$

The oxygen evolution reaction mechanism can be presented based on the following reactions:

(1) $OH^- \rightarrow (OH)_{ads} + e^-$

(2) $(OH^-)_{ads} + OH^- \rightarrow (O^-)_{ads} + H_2O$

(3) $(O^-)_{ads} \rightarrow (O)_{ads} + e^-$

(4) $(O)_{ads} \rightarrow O_2 \uparrow$

In order to express potential in terms of the oxygen overpotential, $\eta$ (when the reference electrode is Ag/AgCl electrode), can be estimated using equation (2) [36]:

$$\eta = E_{meas} - E_{rev} \quad (2)$$

Whereas, $E_{meas}$ is the measured electrode potential and $E_{rev}$ is the reversible electrode potential. For the OER ($E_{rev}$ = 1.23 – 0.059 pH) vs. SHE, at pH 13 (0.1M KOH) $E_{rev}$ = 0.463 V vs. SHE. When the reference electrode is Ag/AgCl electrode in the same solution as the working anode $E_{rev}$ = 0.266 V. Clearly, in this case $\eta$ is related to the voltage, $E_{meas}$, measured on the Ag/AgCl scale as follows:

$$\eta = E_{meas} - 0.266 \text{ V} \quad (3)$$

Table 1 lists the oxygen evolution overpotentials ($\eta$) at the Ag-$TiO_2$/GCE in 0.1 M KOH at various current densities. As observed, the values of $\eta$ increase with the increase in current density.

**Table 1.** Oxygen evolution overpotential, shift potential and the rate of energy saving at the GC electrode obtained after the modification with Ag-$TiO_2$ nanoparticles at various current densities.

| I (mA $cm^{-2}$) | η (mV) | $\Delta E_a$ (mV) | $P_a$ (KWh $kg^{-1}$) |
|---|---|---|---|
| 2 | 454 | 430 | 11.5 |
| 5 | 557 | 480 | 12.8 |
| 7 | 608 | 540 | 14.4 |
| 10 | 650 | - | - |
| 20 | 735 | - | - |
| 30 | 1006 | - | - |

*3.6. Energy savings*

The values for the rate of power savings of oxygen gas were calculated and listed in Table 1. The significant decrease in the potential obtained after GCE modification with Ag-$TiO_2$ corresponds to a reduction in the rate of energy consumption at the anode and consequently, decreases the energy consumption in the overall process. The energy saving at the anode is given by equation (4) [36]:

$$P_{(a)} = \Delta E_{(a)} F / 3600 \quad (4)$$

Whereas $\Delta E_{(a)}$ is anodic potential shift at a current density and $P_{(a)}$ is the KWh per kg of oxygen gas. The value of $P_{(a)}$ calculated at different current densities is listed in Table 1. The observed power savings of oxygen gas of our designed modified electrode was compared with those already reported in papers [30, 36-38]. Moreover, the trapping effect of the profusely generated $O_2$ gas bubbles at the modified electrode with Ag-$TiO_2$ is very low and the values of $P_{(a)}$ increase with the increase in current density. Further, the present modified electrode was highly stable and no tedious procedure was involved in electrode modification.

## 4. CONCLUSION

In summary, we demonstrated a facile method to synthesize Ag-doped $TiO_2$ nanoparticles by sol-gel method. XRD results show the formation of Ag-$TiO_2$ nanoparticles with an average crystallite size of 11 nm. To investigate the catalytic efficiency of Ag-$TiO_2$, the oxygen evolution reaction (OER) was studied using the deposited film of Ag-$TiO_2$ on glassy carbon electrode in alkaline media using LSV. The OER was significantly enhanced upon modification of the electrode with Ag-$TiO_2$, as demonstrated by a negative shift in the LSV curves at the Ag-$TiO_2$/GCE compared to that obtained using bare GCE. The low cost and stability of the modified electrode make it a promising candidate in the industrial water electrolysis process.

ACKNOWLEDGEMENT
This work was supported by the University of Malaya Research Grant (UMRG RP022-2012A).

*Conflict of Interests*
The authors declare that there is no conflict of interests regarding the publication of this paper.

**References**


1. Z.-Z. Gu, A. Fujishima and O. Sato, *Applied Physics Letters*, 85 (2004) 5067.
2. L. Brunet, D. Y. Lyon, E. M. Hotze, P. J. J. Alvarez and M. R. Wiesner, *Environmental science & technology*, 43 (2009) 4355–60.
3. M. Smits, C.K. Chan, T. Tytgat, B. Craeye, N. Costarramone, S. Lacombe and S. Lenaerts, *Chemical Engineering Journal*, 222 (2013) 411–418.
4. A. Linsebigler, G. Lu, and J. Y. Jr, *Chemical Reviews* 95 (1995) 735–758.
5. U. I. Gaya and A. H. Abdullah, *Journal of Photochemistry and Photobiology C: Photochemistry Reviews*, 9 (2008) 1–12.
6. S. N. Habisreutinger, L. Schmidt-Mende and J. K. Stolarczyk, *Angewandte Chemie*, 52 (2013) 7372–408.
7. A. A. Ismail and D. W. Bahnemann, *Journal of Materials Chemistry*, 21(2011) 11686.
8. K. Nagaveni, M. S. Hegde, N. Ravishankar, G. N. Subbanna and G. Madras, *Langmuir : the ACS journal of surfaces and colloids*, 20 (2004) 2900–7.
9. Z. Miao, D. Xu, J. Ouyang, G. Guo, X. Zhao and Y. Tang, *Nano Letters*, 2 (2002)717–720.
10. K. Ding, Z. Miao, Z. Liu, Z. Zhang, B. Han, G. An, S. Miao and Y. Xie, *Journal of the American Chemical Society*, 129 (2007) 6362–3.
11. Y. Zhu, H. Li, Y. Koltypin, Y. R. Hacohen and A. Gedanken, *Chemical communications*, 17 (2001) 2616-2617.
12. M. Zhang, Y. Bando and K. Wada, *Journal of materials science letters*, 20 (2001) 167–170.
13. W. Choi, A. Termin and M. R. Hoffmann, *The Journal of Physical Chemistry*, 98 (1994)13669–13679.
14. Y. Choi, T. Umebayashi and M.Yoshikawa, *Journal of Materials Science*, 39 (2004) 1837–1839.
15. J. Zhang, Y. Wu, M. Xing, S. A. K. Leghari and S. Sajjad, *Energy & Environmental Science*, 3 (2010) 715.
16. B. Liu, H. Chen and C. Liu, S.C. Andrews, C. Hahn and P. Yang, *Journal of the American Chemical Society*, 135 (2013) 9995–9998.
17. S. Ardo and G. J. Meyer, *Chemical Society reviews*, 38 (2009) 115–64.
18. S. G. Kumar and L. G. Devi, *The journal of physical chemistry. A*, 115 (2011) 13211–41.
19. B. Palanisamy, C. M. Babu, B. Sundaravel, S. Anandan and V. Murugesan, *Journal of hazardous materials*, 252-253 (2013) 233–42.
20. K. Ubonchonlakate, L. Sikong and F. Saito, *Procedia Engineering*, 32 (2012) 656–662.
21. D. Guin and S. Manorama, *The Journal of Physical Chemistry C*, 111 (2007)13393–13397.
22. N. Sobana, M. Muruganadham and M. Swaminathan, *Journal of Molecular Catalysis A: Chemical*, 258 (2006)124–132.
23. M. K. Seery, R. George, P. Floris and S. C. Pillai, *Journal of Photochemistry and Photobiology A: Chemistry*, 189 (2007) 258–263.
24. C. He, Y.Yu, X. Hu and A. Larbot, *Applied Surface Science*, 200 (2002) 2–10.
25. A. Fujishima, X. Zhang and D.Tryk, *International Journal of Hydrogen Energy*, 32 (2007) 2664–2672.
26. K. Shankar, J. I. Basham, N. K. Allam, O. K. Varghese, G. K Mor., X. , J. A. Seabold, K. S. Choi and C. A. Grimes, *J. Phys. Chem. C*, 113 (2009) 6327–6359.
27. H.-C. Chien, W.-Y. Cheng, Y.-H. Wang, T.-Y. Wei and S.-Y. Lu, *Journal of Materials Chemistry*, 21 (2011) 18180.
28. J. A. Koza, Z. He, A. S. Miller and J. A. Switzer, *Chemistry of Materials*, 24 (2012) 3567–3573.

29. K. M. Papazisi, A.Siokou, S. Balomenou and D. Tsiplakides, *International Journal of Hydrogen Energy*, 37 (2012) 16642–16648.
30. Sadiek, I. M., Mohammad, A. M., El-Shakre, M. E. & El-Deab, M. S. *International Journal of Hydrogen Energy* 37, 68–77 (2012).
31. F. Chekin, S. Bagheri and S. A. Hamid, *Sensors & Actuators: B. Chemical*,177 (2013) 898–903.
32. S. Bagheri, K. Shameli and S. A. Hamid, *Journal of Chemistry*, 2013 (2012) 1–5.
33. R. Tom, A. Nair, N. Singh and M. Aslam, *Langmuir*, 19 (2003) 3439–3445.
34. M. M. Khan, S. A. Ansari, J. Lee and M. H. Cho, *Materials science & engineering. C, Materials for biological applications*, 33 (2013) 4692–9.
35. E. Laviron, *J. Electroanal Chem*, 100 (1979) 263–270.
36. I. Sadiek and A. Mohammad, *International journal of electrochemical science*, 7 (2012) 3350–3361.
37. S. Bagheri, F. Chekin and S. A. Hamid, *Journal of the Chinese Chemical Society*, 61 (2014) 702-706.
38. A. M. Fundo and L. M. Abrantes, *Journal of Electroanalytical Chemistry*, 600 (2007) 63–79.